RSC Advances

PAPER

View Article Online
View Journal | View Issue

Check for updates

Cite this: *RSC Adv.*, 2019, **9**, 20852

Constructing "breathing" dynamic skeletons with extra π-conjugated adsorption sites for iodine capture†

Lixin Xia,[a] Dongqi Yang,[a] Hongcui Zhang,[a] Qian Zhang,[a] Naishun Bu,[b] Peng Song,[c] Zhuojun Yan*[a] and Ye Yuan*[d]

Received 13th March 2019
Accepted 24th June 2019

DOI: 10.1039/c9ra01904a

rsc.li/rsc-advances

Radioiodine (^{129}I and ^{131}I) emission from the nuclear waste stream has aroused enormous apprehension because of its quick diffusion and radiological contamination. Conventional porous adsorbents such as zeolites and carbon with rigid skeletons and constant pore volumes reveal a limited performance for reliable storage. Here, a series of soft porous aromatic frameworks (PAFs) with additional π-conjugated fragments is disclosed to serve as physicochemical stable media. Due to the flexibility of the tertiary amine center, the PAF products provide sufficient space for the binding sites, and thus exhibit a considerable capability for iodine capture from both gaseous and soluble environments. The obtained capacity of PAFs is *ca.* 1.6 times higher than that of PAF-1 which possesses similar aromatic constituents featuring an ultra-large specific surface area (BET = 5600 m^2 g^{-1}). The novel paradigm of dynamic frameworks is of fundamental importance for designing adsorbents to treat environmental pollution issues.

Open Access Article. Published on 03 July 2019. Downloaded on 7/20/2025 3:39:58 AM.
This article is licensed under a Creative Commons Attribution-NonCommercial 3.0 Unported Licence.

With the rapid development of the nuclear industry, a large amount of volatile radionuclides (^{129}I, ^{131}I, ^{3}H, ^{85}Kr *etc.*) accompanying nuclear fission are effused into the atmosphere.[1] Radioiodine with high volatility and long radioactive half-life (1.57×10^7 years) attracts particular attention because its sustained pernicious effects on human metabolism ultimately result in an increased incidence of thyroid cancer.[2–4] In this regard, great efforts have been focused on adsorbents to effectively capture and store radioactive iodine for safety and accessibility in the use of nuclear energy.[5,6] Typical nuclear fuel processing conditions are under ambient pressure and 350 K where iodine exists as a coagulative vapor (diameter 5.4 Å).[7] Therefore, iodine uptake in porous materials mostly depends on the binding sites and pore volume.[8] However, the traditional adsorbents including zeolites, carbon, and inorganic–organic hybrid porous materials (MOFs, PCPs *etc.*) possess a narrow pore size and finite volume in their rigid skeletons.[9–19] Their settled pore space can be occupied by iodine as the maximum accessibility of 50%, which generates confined iodine capacity.[7,20] To achieve zero emission of radioactive vapors, the development of high-performance porous materials is desperately urgent.

Organic porous frameworks constructed by organic building units through covalent bonds are emerging as novel porous solids.[21–27] Due to the low density, high stability, and large surface area, these functional products have made a probable promise in the field of gas storage, energy conversion, catalysis, and optoelectronics.[28–36] Porous aromatic frameworks (PAFs) as an amorphous representative are well-known for their stable skeletons and large surface areas.[37] Based on the advanced organic chemistry, one is able to prepare versatile PAFs with tunable organic composition and tailored structure.[38] Their salient characteristics motivate wide interests in the design and synthesis of unique porous skeletons to challenge the traditional rigid frameworks for radioiodine adsorption.

In this contribution, we prepared a class of tertiary amine centered PAF materials (LNU 1–4, LNU represents Liaoning University) *via* a Suzuki coupling reaction. Unlike the traditional porous adsorbents, the N linked aromatic fragments could be distorted and triggered into a "breathing" dynamic skeleton for fitting iodine storage.[39–44] Besides, various π-conjugated units were incorporated into the architecture to serve as adsorption sites. Consequently, the soft PAFs with dynamic architectures render a significant adsorption for iodine molecules and enable cycle use for many times while retaining their high capacity.

As illustrated in Scheme 1, LNU-1, LNU-2, LNU-3, and LNU-4 were synthesized by polycondensation reactions of 4-

[a]*College of Chemistry, Liaoning University, Shenyang 110036, P. R. China. E-mail: zjyan@lnu.edu.cn*

[b]*School of Environmental Science, Liaoning University, Shenyang 110036, P. R. China*

[c]*Department of Physics, Liaoning University, Shenyang 110036, P. R. China*

[d]*Key Laboratory of Polyoxometalate Science of the Ministry of Education, Faculty of Chemistry, Northeast Normal University, Changchun 130024, P. R. China. E-mail: Yuany101@nenu.edu.cn*

† Electronic supplementary information (ESI) available. See DOI: 10.1039/c9ra01904a

This journal is © The Royal Society of Chemistry 2019

Open Access Article. Published on 03 July 2019. Downloaded on 7/20/2025 3:39:58 AM.
This article is licensed under a Creative Commons Attribution-NonCommercial 3.0 Unported Licence.

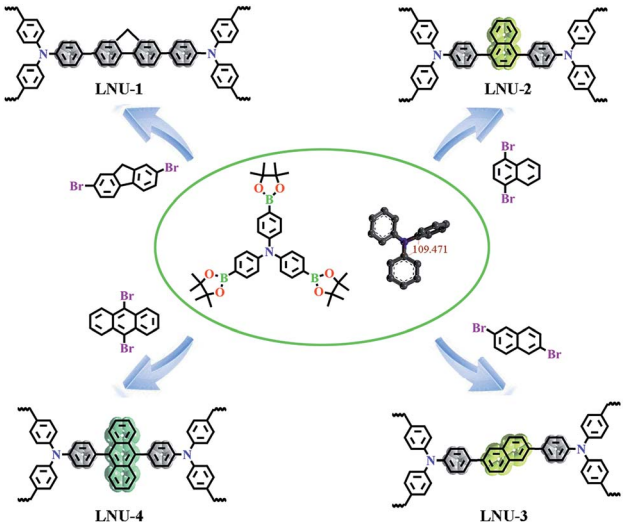

Scheme 1 Synthetic routes for PAF materials LNU-1, LNU-2, LNU-3, and LNU-4 *via* a Suzuki coupling reaction.

(tetramethyl-1,3,2-dioxaborolan-2-yl)-*N*,*N*-bis-[4-(tetramethyl-1,3,2-dioxaborolan-2-yl)phenyl]aniline (BBA) with respective dibromo monomer (2,7-dibromofluorene, 1,4-dibromonaphthalene, 2,6-dibromonaphthalene and 9,10-dibromoanthracene, respectively). According to the Fourier transform infrared spectroscopy (FTIR) spectra (Fig. S1†), the disappearance of C–Br stretching vibration frequency (500 cm^{-1}), C–B vibration band (1417 cm^{-1}), and B–O vibration band (1351 cm^{-1}) from the initial building blocks indicates the completion of cross-coupling reactions and suggests the formation of porous polymers. The structural details of LNU 1–4 networks were also characterized at the molecular level by solid-state ^{13}C NMR spectroscopy (Fig. S2†). The major peaks observed at 135–150 ppm could be assigned to the C substituted aromatic carbons and signals in the range of 120–135 ppm are ascribed to the H coupled aromatic carbons, respectively. Powder X-ray diffraction (PXRD) pattern (Fig. S3†) shows that all PAF samples possess no long-range ordered structure. Scanning electron microscopy (SEM) indicates these resultants are composed of aggregated spheres in micrometer size (Fig. S4†). The worm-like patterns from transmission electron microscopy (TEM) manifest the amorphous textures of LNU 1–4 which is coincident with the PXRD conclusion (Fig. S5†).

The stability and porosity of adsorbents are critical factors for the practical molecular storage application. The four polymers are stable up to 350 °C assessed by thermogravimetric analysis (TGA) in air atmosphere (Fig. S6†). Also there is no weight loss after immersing PAF powders into a variety of common organic solvents, such as DMF, THF, acetone, and $CHCl_3$, respectively, proving the excellent chemical stability of PAFs. The porosities of LNU 1–4 products were evaluated by nitrogen gas adsorption and desorption experiments at 77 K. As shown in Fig. S7,† all resultants show almost no gas sorption at relatively low pressure (P/P_0 < 0.9), and show Type-III isotherms indicating the weak adsorbate–adsorbent interactions.[45,46] The specific surface areas calculated by the BET equation are 26, 20, 30, and 24 $m^2\ g^{-1}$ for LNU-1, LNU-2, LNU-3, and LNU-4, respectively. Meanwhile, the CO_2 isotherms at 273 K and 298 K reveal a typical CO_2 adsorption behaviour (Fig. S8†). As illustrated from CO_2 desorption, all four LUN materials show a hysteretic behavior, which together with the relatively large capacity is the typical character of "breathing" adsorbents. This result suggests that the adsorption mechanism of LNUs preceeds the guest-responsive structural rearrangements and realized the "dynamic" skeletons.[47–49] This phenomenon is attributed to that the N linked aromatic fragments could be distorted leading to a soft skeleton which tends to collapse into a dense, non-porous solid.[50,51]

The traditional rigid adsorbents with a constant porosity exhibit the limited iodine capacity, such as porous silver-doped zeolite mordenite (Ag-MOR), carbon (Cg-5P), and zeolitic imidazolate framework-8 (ZIF-8) possess the slight iodine capacities of 0.07, 0.28, and 1.25 g g^{-1}, respectively.[7] For purposes of comparison, the novel PAF materials with excellent stability and soft architecture were carried out the iodine enrichment experiments by exposing the powder samples into iodine vapor. As shown in Fig. 1 and S9,† LNU-1 without accessible porosity for N_2 molecules could adsorb 2.49 g g^{-1} iodine molecules. As a reference, PAF-1 possesses similar chemical constituents of multiple benzene rings as LNU-1, but a carbon center and high porosity (BET surface area = 5600 $m^2\ g^{-1}$), which only adsorbs 1.86 g g^{-1} iodine.[52] As known, the expanded conjugated network together with the electron-rich characteristic of triphenylamine units possesses strong affinity with I_2 molecules.[15,19,52] For non-porous PAF skeleton (LNU-1), this outstanding iodine uptake implies that the dense structure generates a specific dynamic configuration transformation and is triggered into a "breathing" state due to the flexibility of triphenylamine

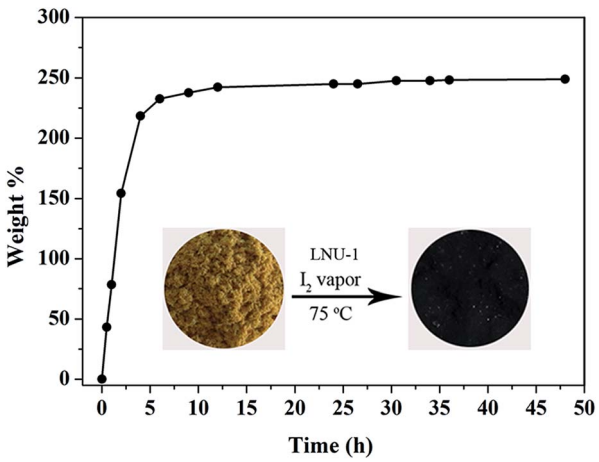

Fig. 1 Iodine uptake of the LNU-1 as a function of exposure time. Photograph for PAF powder LNU-1 before and after iodine capture (inset).

Open Access Article. Published on 03 July 2019. Downloaded on 7/20/2025 3:39:58 AM.
This article is licensed under a Creative Commons Attribution-NonCommercial 3.0 Unported Licence.

fragment, which favours the access and storage of iodine molecules.[51,53,54]

To confirm this speculation, all PAF samples after performed the iodine adsorption procedure were conducted by the TGA analysis. As shown in Fig. 2a, there is a gradual mass loss started from 90 °C and ended at 200 °C, which suggests the strong affinity of iodine with PAF architecture (I_2 boiling point is 184 °C). In addition, we conducted FT-IR, PXRD, and Raman analyses for PAFs after it absorbed I_2 molecules, with the resultant material named PAF-I_2. As illustrated in Fig. 2b, the special bands of C=C and C–H in the phenyl ring change from 1504 and 819 cm^{-1} to 1502 and 822 cm^{-1}, respectively, demonstrating the interaction of aromatic fragments with I_2 molecules.[55] There are no characteristic peaks of elemental iodine in the PXRD patterns compared with I_2 and PAF-I_2 which demonstrates the uniform distribution of iodine molecules in LNU-1 framework (Fig. 2c). Furthermore, the strong peaks at 113 and 173 cm^{-1} recorded by Raman spectroscopy manifest the I_5^- state of adsorbed iodine molecules, which is attributed to the charge transfer between the electron-deficient guest iodine molecules and the electron-rich host network at high coverage (Fig. 2d).[55,56] All these results demonstrate the adsorbed I_2 molecules are uniformly distributed in the PAF architecture suggesting the dynamic configuration transformation of PAF skeleton for fitting the I_2 storage.

This "breathing" dynamic skeleton of LNU-1 prompted us a further investigate to achieve a better performance for radioiodine capture. Various π-conjugated groups including naphthalene and anthracene rings are introduced into the soft framework. In accordance with analysis above, naphthalene based LNU-2 and LNU-3 and anthracene based LNU-4 exhibit a similar "breathing" state which is demonstrated by the TGA, FT-IR, PXRD, and Raman spectra (Fig. S10–S13†). The PAF resultants reveal increased iodine uptake capacities of 2.95 g g^{-1} for LNU-2 and 2.76 g g^{-1} for LNU-3, respectively from 2.49 g g^{-1} for LNU-1. This increased capacity is attributed to the flexible skeleton provides sufficient space for the accessibility of iodine to π-conjugated groups which possess a strong affinity for guest binding through charge transfer.[55–57] Furthermore, two increased FT-IR peaks of conjugated group located at 1258 and 1159 cm^{-1} and the emerging Raman signals at 110 and 175 cm^{-1} demonstrate this charge transfer from the highest occupied molecular orbital (HOMO) of π-conjugated group to the lowest unoccupied molecular orbital (LUMO) of iodine.[45] As to LNU-4 (2.04 g g^{-1} iodine uptake), the anthracene constituent with a similar binding structure as naphthalene group increases the weight of structural unit resulting in the reduced maximum I_2 capacity compared with LNU-2 and LNU-3. Due to the elaborate design, the tertiary amine centered PAF materials express a better performance than the classical microporous polymers including PAF-21 (1.52 g g^{-1}), PAF-23 (2.71 g g^{-1}), pha-HcoP-1 (1.31 g g^{-1}), NAPOP-1 (2.06 g g^{-1}), NIP-CMP (2.02 g g^{-1}), CMPN-3 (2.08 g g^{-1}), and SCMP-1 (1.88 g g^{-1}).[18,19,58–61]

Additionally, the iodine sorption experiments of PAF products were exploited in the iodine containing solution. When PAFs were immersed in a hexane solution of iodine (C = 1000 mg L^{-1}) at room temperature, the dark purple solutions fade gradually to colourless status (Fig. 3a and S14†). This phenomenon indicates the porous frameworks with strong affinity could be utilized to extract iodine molecules from the liquid environments. Notably, the LNU PAFs could be activated upon the thermal treatment at 398 K for 120 min of iodine-captured PAF samples. Also the iodine adsorbed porous skeletons release the guest molecules by immersing the resultants in organic solvents at room temperature (Fig. 3b and S15†). The soft PAF materials are recyclable after the activation at 398 K and 120 min, while retaining a considerable uptake capacity after five cycles (Fig. S16†). All these results demonstrate the tertiary amine centered PAF materials possess tremendous potential for iodine capture application compared to the conventional adsorbents.

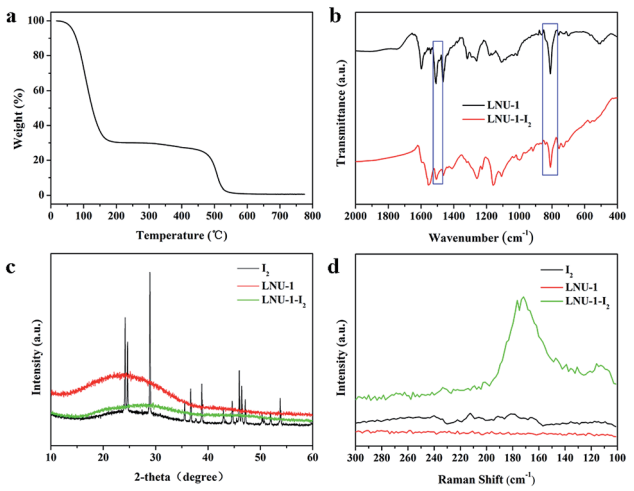

Fig. 2 (a) TGA curve of the iodine adsorbed LNU-1. FT-IR spectra (b), PXRD profiles (c), and Raman spectra (d) of the LNU-1 and iodine adsorbed LNU-1.

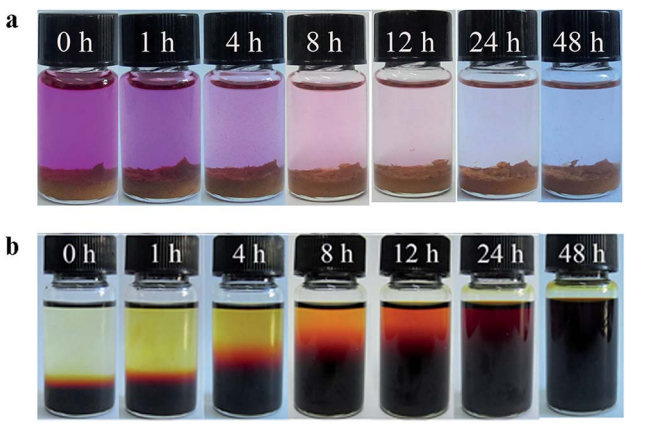

Fig. 3 Photographs indicate the gradual changes in iodine adsorption (a) and desorption (b) processes of LNU-1.

This journal is © The Royal Society of Chemistry 2019

Open Access Article. Published on 03 July 2019. Downloaded on 7/20/2025 3:39:58 AM.
This article is licensed under a Creative Commons Attribution-NonCommercial 3.0 Unported Licence.

Conclusions

In summary, we constructed a series of N centered PAF materials with π-conjugated groups for radioiodine sorption. After exposed into iodine vapor, the specific dynamic skeleton is triggered into a "breathing" state for fitting the iodine storage and provides sufficient space for the iodine access into the π-conjugated adsorption sites. As a consequence, the soft PAFs possess a significant adsorption capability for iodine molecules. Apart from the remarkable adsorption capacity, the success of constructing PAFs with "breathing" dynamic skeleton opens a novel strategy for preparation of novel radioiodine adsorbents.

Conflicts of interest

There are no conflicts to declare.

Acknowledgements

This work was supported by the National Natural Science Foundation of China (21704037, 21671089, and 21604008), the Shenyang Natural Science Foundation of China (F16-103-4-00), Scientific Research Fund of Liaoning Province (LT2017010, 20170540409), Startup Foundation for Doctors of Liaoning Province (20170520069), the Open Project of State Key Laboratory of Urban Water Resource and Environment, Harbin Institute of Technology (ES201809), the Open Research Fund of State Key Laboratory of Estuarine and Coastal Research (SKLEC-KF201713), and Natural Science Foundation of Jilin Province of China (20180520144JH).

Notes and references

1 Z. J. Yin, S. Q. Xu, T. G. Zhan, Q. Y. Qi, Z. Q. Wu and X. Zhao, *Chem. Commun.*, 2017, **53**, 7266–7269.
2 G. Steinhauser, *Environ. Sci. Technol.*, 2014, **48**, 4649–4663.
3 S. Xu, S. Freeman, X. L. Hou, A. Watanabe, K. Yamaguchi and L. Y. Zhang, *Environ. Sci. Technol.*, 2013, **47**, 10851–10859.
4 Y. Chen, F. G. Zhang and Z. M. Xue, *J. Mol. Liq.*, 2016, **223**, 202–208.
5 B. J. Riley, J. D. Vienna, D. M. Strachan, J. S. McCloy and J. L. Jerden, *J. Nucl. Mater.*, 2016, **470**, 307–312.
6 K. W. Chapman, P. J. Chupas and T. M. Nenoff, *J. Am. Chem. Soc.*, 2010, **132**, 8897–8899.
7 P. Wang, Q. Xu, Z. Li, W. Jiang, Q. Jiang and D. Jiang, *Adv. Mater.*, 2018, 1801991–1801997.
8 R. Krishna, *J. Phys. Chem. C*, 2009, **113**, 19756–19781.
9 J. T. Hughes, D. F. Sava, T. M. Nenoff and A. Navrotsky, *J. Am. Chem. Soc.*, 2013, **135**, 16256–16259.
10 B. J. Riley, J. Chun, J. V. Ryan, J. Matyas, X. S. Li, D. W. Matson, S. K. Sundaram, D. M. Strachana and J. D. Vienna, *RSC Adv.*, 2011, **1**, 1704–1715.
11 K. S. Subrahmanyam, C. D. Malliakas, D. Sarma, G. S. Armatas, J. Wu and M. G. Kanatzidis, *J. Am. Chem. Soc.*, 2015, **137**, 13943–13948.
12 X. R. Zhang, I. D. Silva, H. G. W. Godfrey, S. K. Callear and S. A. Sapchenko, *J. Am. Chem. Soc.*, 2017, **139**, 16289–16296.
13 D. F. Sava, K. W. Chapman, M. A. Rodriguez, J. A. Greathouse, P. S. Crozier, H. Zhao, P. J. Chupas and T. M. Nenoff, *Chem. Mater.*, 2013, **25**, 2591–2596.
14 N. X. Zhu, C. W. Zhao, J. C. Wang, Y. A. Li and Y. B. Dong, *Chem. Commun.*, 2016, **52**, 12702–12705.
15 Q. Q. Dang, X. M. Wang, Y. F. Zhang and X. M. Zhang, *Polym. Chem.*, 2016, **7**, 643–647.
16 H. Li, X. S. Ding and B. H. Han, *Chem.–Eur. J.*, 2016, **22**, 11863–11868.
17 Y. F. Chen, H. X. Sun, R. X. Yang, T. T. Wang, C. J. Pei, Z. T. Xiang, Z. Q. Zhu, W. D. Liang, A. Li and W. Q. Deng, *J. Mater. Chem. A*, 2015, **3**, 87–91.
18 Z. J. Yan, Y. Yuan, Y. Y. Tian, D. Zhang and G. S. Zhu, *Angew. Chem., Int. Ed.*, 2015, **54**, 12733–12737.
19 X. Qian, Z. Q. Zhu, H. X. Sun, F. Ren, P. Mu, W. D. Liang, L. H. Chen and A. Li, *ACS Appl. Mater. Interfaces*, 2016, **8**, 21063–21069.
20 Q. Sun, B. Aguila and S. Q. Ma, *Trends in Chemistry*, 2019, **1**, 292–303.
21 S. Y. Ding and W. Wang, *Chem. Soc. Rev.*, 2013, **42**, 548–568.
22 Q. Xu, S. Dalapati and D. Jiang, *ACS Cent. Sci.*, 2016, **2**, 586–587.
23 C. R. Mulzer, L. Shen, R. P. Bisbey, J. R. McKone, N. Zhang, H. D. Abruña and W. R. Dichtel, *ACS Cent. Sci.*, 2016, **2**, 667–673.
24 N. B. McKeown and P. M. Budd, *Chem. Soc. Rev.*, 2006, **35**, 675–683.
25 A. I. Cooper, *ACS Cent. Sci.*, 2017, **3**, 544–553.
26 Y. G. Zhang and S. N. Riduan, *Chem. Soc. Rev.*, 2012, **41**, 2083–2094.
27 B. J. Smith, L. R. Parent, A. C. Overholts, P. A. Beaucage, R. P. Bisbey, A. D. Chavez, N. Hwang, C. Park, A. M. Evans, N. C. Gianneschi and W. R. Dichtel, *ACS Cent. Sci.*, 2017, **3**, 58–65.
28 M. Carta, R. Malpass-Evans, M. Croad, Y. Rogan, J. C. Jansen, P. Bernardo, F. Bazzarelli and N. B. McKeown, *Science*, 2013, **339**, 303–307.
29 C. J. Doonan, D. J. Tranchemontagne, T. G. Glover, J. R. Hunt and O. M. Yaghi, *Nat. Chem.*, 2010, **2**, 235–238.
30 J. Weber and A. Thomas, *J. Am. Chem. Soc.*, 2008, **130**, 6334–6335.
31 R. W. Tilford, S. J. Mugavero, P. J. Pellechia and J. J. Lavigne, *Adv. Mater.*, 2008, **20**, 2741–2746.
32 R. Schmid and M. Tafipolsky, *J. Am. Chem. Soc.*, 2008, **130**, 12600–12601.
33 S. Kandambeth, A. Mallick, B. Lukose, M. V. Mane, T. Heine and R. Banerjee, *J. Am. Chem. Soc.*, 2012, **134**, 19524–19527.
34 S. Demir, N. Brune, J. F. V. K. Humbeck, J. A. Mason, T. V. Plakhova, S. Wang, G. Tian, S. G. Minasian, T. Tyliszczak, T. Yaita, T. Kobayashi, S. N. Kalmykov, H. Shiwaku, D. K. Shuh and J. R. Long, *ACS Cent. Sci.*, 2016, **2**, 253–265.
35 A. G. Slater, P. S. Reiss, A. Pulido, M. A. Little, D. L. Holden, L. Chen, S. Y. Chong, B. M. Alston, R. Clowes, M. Haranczyk,

Open Access Article. Published on 03 July 2019. Downloaded on 7/20/2025 3:39:58 AM.
This article is licensed under a Creative Commons Attribution-NonCommercial 3.0 Unported Licence.

M. E. Briggs, T. Hasell, G. M. Day and A. I. Cooper, *ACS Cent. Sci.*, 2017, **3**, 734–742.
36 Q. Sun, S. Ma, Z. Dai, X. Meng and F. S. Xiao, *J. Mater. Chem. A*, 2015, **3**, 23871–23875.
37 Y. Yuan and G. Zhu, *ACS Cent. Sci.*, 2019, **5**, 409–419.
38 S. Das, P. Heasman, T. Ben and S. L. Qiu, *Chem. Rev.*, 2017, **117**, 1515–1563.
39 Y. Yuan, Y. J. Yang, X. J. Ma, Q. H. Meng, L. L. Wang, S. Zhao and G. S. Zhu, *Adv. Mater.*, 2018, **30**, 1706507.
40 Y. Yuan, Y. J. Yang, M. Faheem, X. Q. Zou, X. J. Ma, Z. Y. Wang, Q. H. Meng, L. L. Wang, S. Zhao and G. S. Zhu, *Adv. Mater.*, 2018, **30**, 1800069.
41 Y. J. Sheng, Q. B. Chen, J. Y. Yao, Y. X. Lu, H. L. Liu and S. Dai, *Angew. Chem., Int. Ed.*, 2016, **55**, 3378–3381.
42 A. D. G. Firmino, R. F. Mendes, M. M. Antunes, P. C. Barbosa, S. M. F. Vilela, A. A. Valente, F. M. L. Figueiredo, J. P. C. Tomé and F. A. A. Paz, *Inorg. Chem.*, 2017, **56**, 1193–1208.
43 T. Tahier and C. L. Oliver, *CrystEngComm*, 2017, **19**, 3607–3618.
44 B. Mu, F. Li, Y. G. Huang and K. S. Walton, *J. Mater. Chem.*, 2012, **22**, 10172–10178.
45 F. L. Zhao, A. J. Dong, L. D. Deng, R. W. Guo and J. H. Zhang, *Polym. Chem.*, 2019, **10**, 2436–2446.
46 M. Alhamami, H. Doan and C. H. Cheng, *Materials*, 2014, **7**, 3198–3250.
47 C. H. Lee, M. R. Tsai, Y. T Chang, L. L. Lai, K. L. Lu and K. L. Cheng, *Chem.–Eur. J.*, 2013, **19**, 10573–10579.
48 A. Schneemann, P. Vervoorts, I. Hante, M. Tu, S. P. Wannapaiboon, C. Sternemann, M. Paulus, D. C. Florian Wieland, S. Henke and R. A. Fischer, *Chem. Mater.*, 2018, **30**, 1667–1676.
49 X. L. Wu, F. Luo, G. M. Sun, A. M. Zheng, J. Zhang, M. B. Luo, W. Y. Xu, Y. Zhu, X. M. Zhang and S. Y. Huang, *ChemPhysChem*, 2013, **14**, 3594–3599.
50 A. K. Mandal, M. Suresh, P. Das and A. Das, *Chem.–Eur. J.*, 2012, **18**, 3906–3917.
51 V. A. Davankov and M. P. Tsyurupa, *React. Polym.*, 1990, **13**, 27–42.
52 F. Ren, Z. Q. Zhu, X. Qian, W. D. Liang, P. Mu, H. X. Sun, J. H. Liu and A. Li, *Chem. Commun.*, 2016, **52**, 9797–9800.
53 C. Zhao, C. S. Diercks, C. Zhu, N. Hanikel, X. Pei and O. M. Yaghi, *J. Am. Chem. Soc.*, 2018, **140**, 16438–16441.
54 C. Wang, Y. Wang, R. Ge, X. Song, X. Xing, Q. Jiang, H. Lu, C. Hao, X. Guo, Y. Gao and D. Jiang, *Chem.–Eur. J.*, 2018, **24**, 585–589.
55 C. Y. Pei, T. Ben, S. X. Xu and S. L. Qiu, *J. Mater. Chem. A*, 2014, **2**, 7179–7187.
56 L. Lin, H. D. Guan, D. L. Zou, Z. J. Dong, Z. Liu, F. F. Xu, Z. G. Xie and Y. X. Li, *RSC Adv.*, 2017, **7**, 54407–54415.
57 H. Xu, S. S. Tao and D. L. Jiang, *Nat. Mater.*, 2016, **15**, 722–726.
58 Y. Z. Liao, J. Weber, B. M. Mills, Z. H. Ren and C. F. J. Fau, *Macromolecules*, 2016, **49**, 6322–6333.
59 J. Y. Weng, Y. L. Xu, W. C. Song and Y. H. Zhang, *J. Polym. Sci., Part A: Polym. Chem.*, 2016, **15**, 1724–1730.
60 L. Q. Xu, L. P. Guo, G. S. Hu, J. H. Chen, X. Hu, S. L. Wang, W. Dai and M. H. Fan, *RSC Adv.*, 2015, **5**, 37964–37969.
61 X. Qian, B. Wang, Z. Q. Zhu, H. X. Sun, F. Ren, P. Mu, C. H. Ma, W. D. Liang and A. Li, *J. Hazard. Mater.*, 2017, **338**, 224–232.

This journal is © The Royal Society of Chemistry 2019